HHS Public Access

Author manuscript

J Neurosurg. Author manuscript; available in PMC 2017 May 06.

Published in final edited form as:

J Neurosurg. 2016 March ; 124(3): 675–686. doi:10.3171/2015.1.JNS141571.

Structural and biochemical abnormalities in the absence of acute deficits in mild primary blast-induced head trauma

Michael K. Walls, MS[1,*], **Nicholas Race, BS**[2], **Lingxing Zheng, PhD**[1,2], **Sasha M. Vega-Alvarez, MS**[1], **Glen Acosta, MS**[1], **Jonghyuck Park, PhD**[1,2], and **Riyi Shi, MD, PhD**[1,2]

[1]Department of Basic Medical Sciences, College of Veterinary Medicine

[2]Weldon School of Biomedical Engineering, Purdue University, West Lafayette, Indiana

Abstract

OBJECTIVE—Blast-induced neurotrauma (BINT), if not fatal, is nonetheless potentially crippling. It can produce a wide array of acute symptoms in moderate-to-severe exposures, but mild BINT (mBINT) is characterized by the distinct absence of acute clinical abnormalities. The lack of observable indications for mBINT is particularly alarming, as these injuries have been linked to severe long-term psychiatric and degenerative neurological dysfunction. Although the long-term sequelae of BINT are extensively documented, the underlying mechanisms of injury remain poorly understood, impeding the development of diagnostic and treatment strategies. The primary goal of this research was to recapitulate primary mBINT in rodents in order to facilitate well-controlled, long-term investigations of blast-induced pathological neurological sequelae and identify potential mechanisms by which ongoing damage may occur postinjury.

METHODS—A validated, open-ended shock tube model was used to deliver blast overpressure (150 kPa) to anesthetized rats with body shielding and head fixation, simulating the protective effects of military-grade body armor and isolating a shock wave injury from confounding systemic injury responses, head acceleration, and other elements of explosive events. Evans Blue–labeled albumin was used to visualize blood-brain barrier (BBB) compromise at 4 hours postinjury. Iba1 staining was used to visualize activated microglia and infiltrating macrophages in areas of peak BBB compromise. Acrolein, a potent posttraumatic neurotoxin, was quantified in brain tissue by immunoblotting and in urine through liquid chromatography with tandem mass spectrometry at 1, 2, 3, and 5 days postinjury. Locomotor behavior, motor performance, and short-term memory were

Correspondence: Riyi Shi, Department of Basic Medical Sciences, Weldon School of Biomedical Engineering, Purdue University, 404 S. University St., West Lafayette, IN 47907. riyi@purdue.edu.

*Messrs. Walls and Race contributed equally to this work.

Disclosure

This work was supported in part by the Indiana State Department of Health (Grant No. 204200 to R.S.), National Institutes of Health (Grant No. NS073636 to R.S.), and Indiana CTSI Collaboration in Biomedical Translational Research (CBR/CTR) Pilot Program Grant (Grant No. RR025761 to R.S.). Funding for the LSM710 was provided by NIH NCRR Shared Instrumentation (Grant No. 1 S10 RR023734-01A1).

Author Contributions

Conception and design: Shi, Walls. Acquisition of data: all authors. Analysis and interpretation of data: all authors. Drafting the article: Shi, Walls, Race. Critically revising the article: Shi, Race. Reviewed submitted version of manuscript: Shi, Race. Approved the final version of the manuscript on behalf of all authors: Shi. Statistical analysis: Shi, Walls, Race. Administrative/technical/material support: Shi. Study supervision: Shi.

assessed with open field, rotarod, and novel object recognition (NOR) paradigms at 24 and 48 hours after the blast.

RESULTS—Average speed, maximum speed, and distance traveled in an open-field exploration paradigm did not show significant differences in performance between sham-injured and mBINT rats. Likewise, rats with mBINT did not exhibit deficits in maximum revolutions per minute or total run time in a rotarod paradigm. Short-term memory was also unaffected by mBINT in an NOR paradigm. Despite lacking observable motor or cognitive deficits in the acute term, blast-injured rats displayed brain acrolein levels that were significantly elevated for at least 5 days, and acrolein's glutathione-reduced metabolite, 3-HPMA, was present in urine for 2 days after injury. Additionally, mBINT brain tissue demonstrated BBB damage 4 hours postinjury and colocalized neuroinflammatory changes 24 hours postinjury.

CONCLUSIONS—This model highlights mBINT's potential for underlying detrimental physical and biochemical alterations despite the lack of apparent acute symptoms and, by recapitulating the human condition, represents an avenue for further examining the pathophysiology of mBINT. The sustained upregulation of acrolein for days after injury suggests that acrolein may be an upstream player potentiating ongoing postinjury damage and neuroinflammation. Ultimately, continued research with this model may lead to diagnostic and treatment mechanisms capable of preventing or reducing the severity of long-term neurological dysfunction following mBINT.

Keywords

blast-induced neurotrauma; BBB disruption; oxidative stress; acrolein; 3-HPMA; traumatic brain injury; trauma

---

Blast injury, often referred to as the "signature injury of modern warfare," has seen a recent surge of interest in response to the increased incidence of reported head injuries. Approximately 1 in 5 wounded soldiers suffers from traumatic brain injury,[55] and an estimated 52% of those injuries are blast-induced neurotrauma (BINT).[22,62] It is evident that a high proportion of veteran BINT victims, upon their return to civilian life, have difficulty coping with the transition and maintaining relationships and often suffer from posttraumatic stress disorder (PTSD) spectrum deficits or depression.[9,11,13,27,46,51,70] Links between blast injury and neurodegenerative diseases such as chronic traumatic encephalopathy have also been demonstrated. [32,52] Therefore, there is an urgent need to better understand the mechanisms and etiology of these injuries, establish effective diagnostic techniques, offer early intervention, improve outcomes, and reduce BINT-related health problems.

BINT is caused by explosive events and is divided into 4 injury subcategories: primary, secondary, tertiary, and quaternary. "Primary injury" refers solely to impact from a shock wave emanating from the explosion epicenter. "Secondary BINT" refers to penetrating injury from shrapnel and other objects. "Tertiary BINT" is equivalent to classic "impact-acceleration" or "coup-contrecoup" head injuries that result from blast wind–induced head accelerations and blunt collisions with objects. "Quaternary injury" encompasses all other potentially dangerous elements of BINT including heat, chemical exposure, radiation, and so forth. Secondary, tertiary, and quaternary BINTs have all been extensively studied and have well-established mechanisms of injury; however, despite intense research interest, no clear

picture has emerged regarding the mechanisms of initial injury for primary BINT or its subsequent pathological processes.[22,23,62] This is particularly true for mild BINT (mBINT) victims who usually lack auspicious acute motor or other neurological deficits and thus remain unrecognized and untreated for extended periods of time.[13,22,16,62,64,52] Recent human studies have shown that even asymptomatic mBINT victims can suffer significant chemical alterations that may be related to the delayed onset of neurological dysfunction.[33,72,73] These findings highlight the difficulty and importance of early mBINT detection, indicating that missed early diagnosis and a subsequent lack of intervention could lead to serious long-term consequences. Early detection and intervention could potentially mitigate or prevent delayed-onset development of significant neurological dysfunction.

To advance our knowledge in this arena, it is essential to have an animal model that mirrors the human condition and allows for careful interrogation of structural, biochemical, and behavioral phenotypes that result from underlying pathological mechanisms. To this end, in the current investigation we have established a rat model of primary mBINT. Injury-scaling laws between humans and rodents do not exist for primary BINT, nor have the physical parameters of blast-wave intensity (magnitude, duration, and so forth) proven to be the primary determinants of injury severity.[68,76] Therefore, it is imperative that any model of BINT assesses acute postblast outcomes so conclusions can be appropriately drawn within the context of injury severity. The evidence in this paper, to our knowledge, represents the first effort to assign clinically relevant injury classification in a rodent BINT model according to the Centers for Disease Control and Prevention (CDC) injury severity guidelines for humans, a measure necessary to achieve translational relevance.

As is common during the acute, post-mBINT exposure period in humans,[16,64] mBINT-injured rats in our model lacked acute motor or short-term memory deficits in the days following injury. Memory and motor metrics were chosen because of their similarity to current common clinical neurocognitive assessments for suspected brain injury. Despite the rats' asymptomatic appearance in the acute posttrauma period, significant region-specific structural damage to the blood-brain barrier (BBB) and evidence of neuroinflammation was evident and detectable via concurrent local and systemic biochemical assessments. In particular, we detected an increase of acrolein—an established endogenous posttraumatic neurotoxin, perpetuator of oxidative stress, and proinflammatory agent—in the days following injury. Having established and confirmed a mild injury model in which apparent morphological and biochemical injury exists despite asymptomatic behavioral presentation on neurocognitive assessments, we expect that this model will provide an effective avenue to further study primary mBINT injury mechanisms and pursue new diagnostic and therapeutic measures for mBINT.

Methods

Animal Model of Primary BINT

All live animal procedures were conducted under animal use protocols approved by the Purdue University Animal Care and Use Committee. Animals (42 total) were anesthetized with a ketamine and xylazine cocktail (80 and 10 mg/kg, respectively). After verifying the absence of the toe-withdrawal reflex, animals were secured in an open-ended, shock tube–

style blast apparatus with a thin latex band protecting the eyes and ears and a custom acrylic shield covering the body from the base of the skull to the tail to simulate body armor and to prevent pulmonary injury. Head fixation was used to eliminate confounding effects of tertiary blast injury (via blast wind–induced head acceleration) in order to study primary blast injury in isolation. The use of compressed gas for shock wave generation also allowed for the elimination of secondary and quaternary BINT, which result from the use of conventional explosives. In concert, these measures allowed for the isolated investigation of primary mBINT while limiting systemic confounders. One-way ANOVA was used for all statistical analyses with $p < 0.05$ chosen as the threshold for significance.

The platform consisted of a rigid wire grid that allowed the blast wind and shock wave to pass freely beside the animal and simulate a free-field blast exposure. The blast chamber consisted of a custom-built stainless steel loading chamber and chute bolted together with a polyethylene terephthalate (PET) membrane (McMaster-Carr) and O-ring sealed in between. Varying the thickness of the PET membrane allowed for adjustment of blast strength. Compressed nitrogen was used as the driver gas and was delivered to the chamber via a custom-built pneumatic switch control. Although several exposure intensities were characterized, a mild, nonlethal blast was selected for the purposes of this study. The shock tube system is illustrated in Fig. 1. This model was shown to reproducibly generate blast overpressure at multiple levels ranging from 75 to 1200 kPa by varying the distance between the chute opening and the probe and by varying the thickness of the membrane separating the driver and driven sections. A representative pressure recording in Fig. 1D illustrates the 150-kPa blast level used in this study and demonstrates the Friedlander waveform typical of free-field shock waves. The shock wave intensity we used for this in vivo study of mild injury was chosen based on guidance from previous data collected using higher severity, positive control blasts (535–1200 kPa);[20] comparison with literature describing injury/lethality curves for different overpressure amplitudes and durations;[8,17] and postblast evaluation of signs and symptoms that were verified to be consistent with CDC and Department of Defense (DoD) guidelines for mild injury. Overpressure blasts of 150 kPa are consistent with existing blast investigations in rats,[19,68,76,79] which have documented tissue and cellular changes but have not been studied in the context of clinical injury severity or biomarker-based, post-BINT screening tools.

Physical Characterization—Dynamic Pressure Transducers

Blast events were characterized using a DPX101–250 dynamic pressure transducer (Omega Engineering Inc.). Signal acquisition was performed at 200 kHz using a custom LabView virtual interface (National Instruments Corp.). Waveforms for peak overpressure were obtained to verify repeatability and dosing as shown in Fig. 1D.

Behavioral Assessment of Gross Motor and Short-Term Memory Function

Gross motor deficits were examined by 5-minute excursion sessions in an open-field activity box as described by Koob et al.,[41] with video feed motor metric analysis conducted using AnyMaze software (Stoelting Co.). Briefly, the activity was evaluated for distance traveled, average speed, and maximum speed. Additionally, rats were evaluated for locomotion on a rotarod. The rotarod speed increased gradually from 0 to 30 revolutions per minute (rpm)

over 3 minutes and remained at 30 rpm until stopping at the 3-minute, 30-second mark or earlier if the rat fell. Criteria were developed to ensure animals were accustomed to the apparatus and testing before exposure. For pre-BINT training, the rats had to successfully complete 2 out of 3 runs at 30 rpm (top speed). Sham-injured animals (anesthesia and blast noise only without shock wave exposure) were examined in tandem to control for lingering effects of anesthesia in the acute postinjury period. Each motor assessment was conducted at 24 and 48 hours after mBINT for both blast-injured (n = 4) and sham-injured (n = 4) groups.

At 24 and 48 hours after mBINT, short-term memory was assessed through a 5-minute exposure to an object in an open-field activity box followed by a 30-minute rest period. After the rest period, animals were placed back in the open field with 2 objects: the original object (familiar) and a new object (novel). The initial and final placement of the object was randomized within an ANOVA-balanced, complete block design for both objects to eliminate effects of animal place preference. Time spent investigating each object was quantified from video recordings using Any-Maze software for both blast-injured (n = 4) and sham-injured (n = 4) animals. Normal function of short-term memory was indicated by more time spent actively investigating the novel object as compared with the familiar object during the second open-field excursion (after the rest period).[5,10]

Blood-Brain Barrier Integrity Assessment

BBB compromise was assessed by fluorescence microscopy of formaldehyde-fixed brain slices to quantify anatomical distributions of serum albumin extravasation. According to methods adapted from previously published work,[37] Evans Blue (EB) dye was intraperitoneally injected into rats (2 groups [sham and blast injured] of 4 animals) 3 hours before exposure to the blast and allowed to enter the vascular circulation. EB was dissolved in normal saline to produce a 3% (w/v) solution. A noticeable bluish-gray hue in normally pink tissues served as confirmation of vascular EB uptake. Occasional injections of EB into the gut rather than the peritoneal cavity (as evidenced by dark blue/black feces with no noticeable blue hue in normally pink tissues) required a second dose of EB. Following blast exposure, the animals were allowed to recover for 3 hours during which extravascular albumin could accumulate. Animals were then transcardially perfused with oxygenated Krebs solution (approximately 300 ml) until the perfusate ran clear and the liver and lung tissue were pale in color. Immediately afterwards, approximately 60 ml of di-alkylindocarbocyanine (DiI; Life Technologies, Inc.) solution (0.12%) in phosphate-buffered saline (PBS)/ethanol/glucose[43] was perfused, followed by approximately 60 ml of 4% paraformaldehyde in 1× PBS. Brain tissue was extracted and sliced in gross sections approximately 1.5 mm thick for postfixation overnight in 4% paraformaldehyde. Vibratome (Electron Microscopy Sciences) sections were cut 100–200 μm thick and placed in 12-well plates submerged in 1× PBS until subsequent imaging. Imaging was performed within 24 hours of final sectioning and within 48 hours following perfusion.

Laser Confocal Microscopy

Brain slices were imaged on a Zeiss LSM710 (Carl Zeiss) with laser line excitation at 633 nm and 514 nm for EB and DiI, respectively. Emission spectra detection parameters for EB and DiI, respectively, were 634+ nm and 515–632 nm. The following parameters were kept

constant across acquisition sessions: pinhole diameter 213 μm, dwell time 12.61 μsec, laser power (EB:DiI) 13:20, and gain (EB:DiI) 791:786. Image acquisition was performed with the 10× objective with 0.6× zoom with tile-scan parameters adjusted according to the slice area.

Assessment of Activated Microglia and Infiltrating Macrophage Neuroinflammation

Twenty-four hours after blast injury, animals (n = 6; 3 blast-injured and 3 sham-injured rats) were killed through transcardial perfusion with oxygenated Krebs solution, following the same procedure as for the BBB integrity assessment. Following Krebs perfusion, 120 ml of fixative solution (4% paraformaldehyde in 1× PBS) was perfused. The extracted brain tissue was then postfixed for 24 hours at 4°C followed by cryoprotection in a 30% (w/v) sucrose solution until sinking (2–5 days). The tissue was then embedded in optimal cutting temperature compound (OCT; Sakura Corp.) and subsequently stored at −80°C until processing. The embedded brains were coronally sectioned in 25-μm increments on a Thermo Shandon Cryotome FE cryostat, mounted on slides, air-dried for 2 hours, and stored at −20°C. Slides were hydrated in 1× PBS (137 mM NaCl, 2.7 mM KCl, 10 mM Na^2HPO^4, 1.8 mM KH^2PO^4, pH 7.4) for 10 minutes, permeabilized in 0.2% Triton X-100 for 5 minutes, and blocked in 10% normal donkey serum for 2 hours. Slides were incubated in goat polyclonal anti-Iba1 (1:500, Abcam Inc.) diluted in PBS with Tween 20 (PBST) with 1% donkey serum for 2 hours, washed 4 times for 5 minutes with PBS, and then incubated with donkey anti–goat Alexa Fluor 594 (1:500, Jackson ImmunoResearch Laboratories Inc.) diluted in PBST with 1% donkey serum for 1 hour. After 4 washes with 1× PBS, slides were coverslipped with Prolong Gold Antifade Reagent (Life Technologies Inc.), allowed to dry for 1 hour, and stored in the dark at −20°C. Finally, fluorescence imaging was performed on an Olympus (IX51) microscope using a Texas red filter and an Olympus (UHGLGPS) light source at 4× and 20× magnification.

Biochemical Assessment of Acrolein-Lysine Adduct and Acrolein Metabolite 3-HPMA

Changes in acrolein, a known neurotoxin, were assessed in both homogenized brain tissue and excreted urine. Following transcardial perfusion with oxygenated Kreb's solution, brain tissue was removed, and the samples were weighed and homogenized for assessment of acrolein-lysine protein adducts by dot blot analysis as previously described.[80] Urine S-(3-hydroxypropyl)mercapturic acid (3-HPMA) was also collected and quantified, as described in the aforementioned paper. Briefly, urine was collected in standard metabolic collection cages prior to BINT and daily for 3 days following blast exposure. Urine was prepared using solid-phase extraction before liquid chromatography with tandem mass spectrometry (LC-MS/MS) analysis based on previously published methods.[26,80] Levels of 3-HPMA were normalized to urine creatinine levels under the assumption of normal kidney function. In the healthy kidney, a steady concentration of creatinine in urine is observed, enabling a calibration against potentially variable urine concentration. Urine samples were assessed once before injury (pre–blast-injured controls) and then daily for 1–5 days post–blast injury (n = 5 rats total; each rat served as its own control).

Results

Open Field, Rotarod, and Novel Object Recognition Behavioral Assessments

Behavioral analysis of motor function in an open-field activity box at 24 and 48 hours postblast indicated no significant deficits resulting from the blast exposure (Fig. 2). Analyses included average speed, maximum speed, and total distance traveled. No statistically significant differences were found before or after the blast in any of the 3 assessments related to open-field activity (n = 4 animals/group; 2 groups: blast and sham injured).

Rotarod studies also revealed no statistical difference in motor function as assessed by maximum speed and total run time at 24 and 48 hours postblast (Fig. 3; n = 4/group). Prior to injury or sham-injury, rats were trained with a protocol designed to ensure familiarity and ability to complete the full test procedure. Lack of gross motor deficits in the open-field and rotarod tests are consistent with the lack of human motoric deficits in the acute term after mBINT.[16,64,73]

The novel object recognition (NOR) test indicated both blast-injured (n = 4) and sham-injured (n = 4) animals exhibited a normal ability to distinguish familiar objects (FOs) and novel objects (NOs), and their capacity to do so was substantially equivalent to one another at both 24 and 48 hours postinjury with a consistent NO/FO investigation time ratio of approximately 2:1 (Fig. 4). Collectively, no significant motor or short-term memory deficits were detected in the acute postinjury period, consistent with clinically mBINT in humans.[16,64,73]

Laser Confocal Microscopy Evaluation of BB Disruption

Confocal microscopic evaluation of tissue slices showed localized elevations of serum albumin in brain parenchyma. Local extravasations of serum albumin were indicated by fluorescence emission of EB outside of the vasculature (Fig. 5). Regions of greatest extravasation included periventricular areas and cortical regions, but extravasation most consistently occurred contralateral to the dorsal incident blast wave in the ventromedial areas including the medial forebrain bundle, olfactory tubercle, amygdala, and ventral pallidum—areas associated with reward circuitry[29,38,69,71] and motor coordination.[7,18,24] The inset in Fig. 5D (enlarged in Fig. 5F) shows the ventromedial region with pronounced fluorescence in the blast-exposed animal. Note also the less pronounced, yet still elevated, fluorescence around the cortical regions, which is also typical in blast-exposed animals. Fluorescence-level differences for the ventral regions (e.g., Fig. 5E and F) are quantified in the bar graph showing the significant difference between sham-injured and blast-exposed animals ($p < 0.005$, n = 4/group; 2 groups).

Assessment of Activated Microglia and Infiltrating Macrophage Neuroinflammation

Qualitative immunohistochemical assessment of microglial/macrophage inflammation was conducted on blast-exposed (n = 3) and sham-injured (n = 3) animals. Representative images of 25-μm-thick coronal sections of sham-injured (Fig. 6A) and injured (Fig. 6B) rat brains after immunofluorescent staining for the microglial/macrophage marker Iba1 (red) indicate glial activation and/or macrophage infiltration.[63] All images correspond to tissue from the

ventral areas of interest identified in Fig. 5E and F, demonstrating colocalized microvascular damage at 4 hours (Fig. 5) and subsequent neuroinflammation at 24 hours (Fig. 6) after blast exposure. Figure 6A and B is shown at 20× magnification with digitally zoomed insets (right) to highlight the characteristic amoeboid, "activated" [77] morphology of Iba-1+ cells after mBINT as compared with the ramified, "non-activated"[77] morphology of Iba-1+ cells from sham-injured animals. Iba-1 stains activated microglia and infiltrating macrophages from peripheral blood.

Biochemical Assessment of Acrolein-Lysine Adduct and Acrolein Metabolite 3-HPMA

Dot blot analysis using homogenized brain tissue from rats sacrificed at 1 and 5 days postblast indicated significant ($p < 0.001$ and $p < 0.05$, respectively; $n = 5$/group; 3 groups) elevations in acrolein-lysine adducts compared with those in preblast controls (Fig. 7A). By postblast Day 5, although still significantly elevated relative to preblast controls, the acrolein-lysine adducts level had significantly decreased ($p < 0.05$) relative to Day 1 (Fig. 7A). This suggests that oxidative stress is elevated on a subacute timescale in the CNS following blast exposure. A stable acrolein metabolite, 3-HPMA,[80] was analyzed by LC-MS/MS in the urine of blast-exposed animals at 24, 48, and 72 hours postinjury. 3-HPMA, a product of the reaction of acrolein and glutathione,[80] showed significantly elevated levels in the urine at 24 and 48 hours postblast compared with levels in preblast controls ($p < 0.05$). However, at 72 hours postblast, no significant difference was found as compared with that of preblast control animals (Fig. 7B).

Discussion

Establishment of a Clinically Relevant Rat Model of Primary mBINT

In a previously published conference paper,[20] we explored the effects of blasts at several higher intensities, ranging from 535 to 1200 kPa. Although the 535-kPa injury was termed relatively "mild" compared with the higher-intensity injuries in that study, even that intensity level resulted in gross brain hemorrhage, a result consistent with clinically severe injury in humans.[16,20,64] Furthermore, the high rates of immediate postblast mortality and seizures indicated that the injury levels tested exceeded the standard for mild injury intensity.[16] Despite a plethora of studies that have enhanced our understanding of primary blast injury biomechanics and pathophysiology, post-BINT alterations have yet to be studied in the context of injury severity, which requires assessing acute functional neurological outcomes. While physical injury intensity does play a role, it has been documented that physical parameters of the blast wave alone (i.e., overpressure magnitude and duration) do not directly dictate injury severity and cannot be the only consideration when establishing a clinically relevant blast model.[68,76] Due to interspecies variation and differing modes of blast generation between investigators, postblast outcomes must be used to assess BINT severity and verify consistency with accepted guidelines within one's own model. Our selection of the 150-kPa overpressure magnitude and 1.5-msec-duration blast wave was based on our prior work[20] as well as an analysis of previous studies in which post-BINT neuropathological changes had been observed, although clinical evaluation of blast severity via acute postblast behavioral assessments had not been performed.[19,68,75,76,79]

The CDC and DoD classify mBINT with the following characteristics: loss of consciousness (LOC) ≤ 30 minutes, Glasgow Coma Scale score of 13–15 following LOC, posttraumatic amnesia < 24 hours, and no evidence of gross intracranial hemorrhage.[16,64] Acute clinical evaluations for brain injury commonly include neurocognitive assessments of short-term memory and motor function, for which mildly injured patients are often asymptomatic and thus can remain undiagnosed for extended periods of time.[16,64] In the present study, we have established a rat model of primary mBINT lacking gross hemorrhage or acute neuromotor and neurocognitive deficits at 24 and 48 hours postinjury, consistent with the human mBINT experience.[16,64] Despite an absence of apparent damage, mBINT-injured rats demonstrated significant biochemical (elevated acrolein levels) and morphological (BBB damage and microglial activation) abnormalities. Although this damage did not confer a functional behavior change in any of our acute assessments, we hypothesize that these subtle, yet detectable, alterations may play a role in the development of delayed-onset neuropathologies consistently documented in both animal and human mBINT investigations. Specifically, we have noted evidence of BBB breakdown in the ventral portion of the brain with concomitant neuroinflammation, as assessed by IbA-1+ cell staining of activated microglia and infiltrating macrophages. We also report significantly elevated levels of acrolein, a potent endogenous posttraumatic neurotoxin[48,50,67] for at least 5 days post-mBINT. As such, this animal model demonstrates that it is indeed possible to have asymptomatic mBINT presentation with underlying, yet detectable, pathological changes; this model also reproduces some key elements of recently described phenomena of subclinical brain injury observed in human primary mBINT,[16,62,64,73] namely unchanged performance on neuromotor and neurocognitive testing in the acute postinjury period.

Potential for Acrolein and 3-HPMA as Theranostic Biomarkers for BINT

Many biomarkers have been repeatedly tested in the context of BINT. The most popular candidate biomarkers have included serum measurement of both glial activation proteins (MBP, GFAP, and S100β) and proteins linked to neuronal damage (NF-H and NSE).[2] Those biomarkers tested in mBINT injuries have yet to provide substantial evidence of diagnostic or prognostic value, largely because of the restrictive time windows (on the order of hours) during which each marker's expression significantly changes from baseline levels.[2,73] We hypothesize that sustained elevation (on the order of days) of acrolein acts as an upstream mediator and perpetuator of the myriad pathophysiological processes responsible for the development of post-mBINT neuropathologies. As such, we believe acrolein is a deserving target for further exploration of its role in mBINT and demonstrates promising diagnostic potential because of its sustained elevation profile postinjury.

Acrolein is endogenously produced by neurons when they are mechanically injured.[34,50,67] Once elevated in CNS tissue, acrolein can wreak havoc, leading to cell death by directly disrupting membranes, impairing mitochondrial function, perpetuating oxidative stress, and inducing inflammation.[34,47,48] Given acrolein's documented widespread toxic effects in the CNS, we postulate that it may be an upstream player in many of the contributing pathophysiological pathways to post-mBINT brain damage. The connection with acrolein elevation suggests that primary mBINT could potentially contribute to an array of postblast neuropathological events that acrolein is known to be associated with, including direct

damage to neurons, BBB compromise, and proinflammatory cascades.[14,35,42,45,48,50,60,67,74] We have multiple in vitro and in vivo studies demonstrating that acrolein is significantly elevated after traumatic neural injury.[25,34,35,47,49,58,65,66] We and others have also demonstrated that exogenously administered acrolein is directly toxic to neurons and a potent proinflammatory agent.[12,30,40,47–49,59,65,67] Furthermore, we have previously shown that endogenously produced acrolein is capable of reaching toxic levels in other rodent models of neural trauma (spinal cord injury).[34,50,66,80] In those models and other studies in humans, pharmacological reduction of acrolein via acrolein scavengers improves structural and functional outcomes at the cellular and tissue levels, consequently reducing postinjury neurological deficits.[35,36,42,58,78]

In support of its potential role in the diagnosis of mBINT, 1 of the acrolein-detection methods employed in the current study, measurement of stable 3-HPMA in urine, is a noninvasive approach that permits longitudinal monitoring of changes in acrolein levels and subsequent correlation to disease presence and/or progression.[80] With this method, we demonstrated an ability to measure acrolein elevation for at least 2 days post-mBINT, during which rats were asymptomatic on neuromotor and neurocognitive testing. Previous diagnostic biomarker investigations of BINT have used protein or nucleic acid screens that require invasive sampling of blood or cerebrospinal fluid (CSF), a clinical action that would be unwarranted and impractical in mBINT patients who generally appear clinically normal.[2,3,16,33,64] One interesting aspect of the diagnostic value of urine 3-HPMA levels in the present study is that this parameter lost significance by Day 3 postblast, while the acrolein-lysine byproduct in brain lysate remained at significantly elevated levels through Day 5. We propose that the return to baseline levels of urine 3-HPMA, despite ongoing local acrolein-lysine elevation in brain tissue, may in fact be evidence of the local endogenous brain glutathione reserves becoming exhausted and thereby preventing reduction of the acrolein-lysine adducts, while more systemic glutathione reserves contribute to decreasing the 3-HPMA byproduct, as we previously investigated in spinal cord injury (SCI).[80] This hypothesis is supported by the evidence that local glutathione is reduced following traumatic CNS injury.[67] Further examination of this phenomenon is being explored. Another possible explanation for the discrepancy between tissue and urine acrolein levels is simple dilution. Elevated tissue acrolein is diluted when entering the systemic circulation, a much larger volume from which to sample.[80] In this sense, a more sensitive detection method may be able to detect the changes in systemic acrolein levels (via 3-HPMA) beyond 3 days postinjury.

Because of its implication in multiple neuropathological processes, particularly oxidative stress[28,48,50,67,74,78] and inflammation,[4,42,53,74] acrolein could also be an effective upstream therapeutic target to mitigate postblast neuronal damage. Advantages of an acrolein sequestration approach for BINT treatment include a clear, identifiable molecular target for intervention using established evaluation methods and readily available, FDA-approved, effective acrolein scavengers such as hydralazine[35,42] and phenelzine.[78] In addition, because of its known neurotoxicity and the demonstrated correlation between magnitude of elevation and injury severity in other traumatic neuropathological events such as SCI,[35,50,80] elevated acrolein levels could potentially be employed as a diagnostic indication that correlates with the severity of post-BINT secondary injury. This is an avenue that merits further study and is

a target of future investigations. We expect that an acrolein-scavenging approach is not only scientifically sensible but also practically feasible and will likely lead to the development of neuroprotective therapies for BINT that can be translated to the clinic in a timely fashion.

Blood-Brain Barrier Damage and the Potential Role of Acrolein

The observation of post-BINT BBB damage is consistent with work by Garman et al.[31] and Yeoh et al.[79] In the current study, we show histological evidence, based on extravasation of serum albumin through a compromised BBB at 4 hours postinjury, that mBINT induces acute BBB disruption. Interestingly, Garman et al.[31] showed similar contralateral (to blast) elevation in BBB permeability but used a laterally impinging blast injury model. Both Garman et al.[31] and Yeoh et al.[79] recognized that a contralateral injury may be the result of tertiary blast effects due to insufficient head restraint (coup-contrecoup injury); however, as suggested by Garman et al.,[31] it may also be attributed to skull flexure and shock wave implosion around the contralateral side. In our study, with the rat's head fixed in place to prevent tertiary blast effects, the blast struck the dorsum of the rat skull, and the area displaying the greatest structural injury was at the base (ventral side) of the brain, opposite to the incident blast based on our structural analysis (Fig. 5). Therefore, both studies (Garman et al.[31] and ours) showed similar patterns of injury, suggesting similar biomechanics of intracranial tissue deformation and damage contralateral to the blast impact site. Indeed, similar results were also observed in an ex vivo neural compression study in which the highest density of damaged axons were located on the opposite side of contact.[56,57] Further, our investigation revealed that mBINT tissue damage can occur from shock waves alone in the absence of head acceleration. A previous study, Goldstein et al. showed that head fixation eliminated post-BINT spatial memory deficits in the Morris water maze, attributing them to tertiary BINT acceleration-induced effects. [32] Our findings, in tandem with those of Goldstein et al., highlight that primary BINT in isolation can still damage brain tissue despite the apparent absence of injury on common behavioral assessments that successfully detect a combination of primary plus tertiary BINT injuries. These observations further underscore the need for improved acute detection techniques.

The BBB damage profile, consistent with those of our colleagues, illustrates that mechanical damage does occur intracranially at the time of injury in this model. Since acrolein is produced as a result of mechanical damage to the CNS, particularly neural tissue,[35,50,67] it is likely that the mechanical stresses and strains responsible for damaging the BBB also traumatically deform local neural tissue, resulting in consequential elevation of acrolein. Because acrolein can also independently cause cellular damage,[48,50,61] including damage to lipid membranes,[48,67,74] it is likely that acrolein elevation further worsens BBB integrity. In summary, the BBB damage is consistent with and suggests that upregulation of acrolein occurs as a result of direct mechanical damage to brain tissue resulting from BINT. We further suggest that elevated acrolein could exacerbate BBB breakdown. One critical piece of evidence supporting such a notion is that acrolein exposure can lead to destruction of claudin-5 (CLDN5), a critical component of BBB tight junctions.[6,39,54] Furthermore, CLDN5 has recently been shown to be absent from brain microvasculature in the hours following BINT.[1]

Colocalized Alterations in Inflammatory Morphology With BB Damage

Microglia are resident protectors of neural function that, under normal conditions, play a role in homeostasis and immunomodulation of local microenvironments.[44] However, when brain tissue is injured, microglia roles can change as they trim and/or eliminate dying neurons via phagocytosis.[44] A major indicator of such activity is a structural change from a resting state ramified, dendritic appearance (Fig. 6A) to an activated amoeboid morphology with retracted processes (Fig. 6B).[77] Our qualitative neuroinflammation assessment using IbA-1 staining revealed colocalized changes to amoeboid morphology and an increased number of IbA-1+ cells (Fig. 6) within areas of BBB damage (Fig. 5). This finding is consistent with expectations, as microglia have been documented to activate and cluster in proximity to damaged microvessels as a result of leaked blood products, as is consistent with our results.[21] It is important to note that IbA-1 stains both activated microglia and infiltrating peripheral macrophages. [63] While we cannot directly distinguish between the 2 cell types, peripheral macrophage infiltration has also recently been shown to correlate with neuronal death after mechanical disruption of the BBB.[61] Alterations in inflammatory cell density and morphology serve as further confirmation of damaged tissue and provide avenues for further investigation. With acrolein's known ability to initiate and perpetuate proinflammatory pathways, specifically from the macrophage lineages,[4,12,30,40,59] it is possible that sequestration of acrolein will mitigate this upregulation of inflammatory activity.

Conclusions

Altogether, we have developed an animal model for blast injury using a compressed air chamber to deliver rapid, explosive-like, shock-wave exposure that isolates primary BINT from systemic confounders. Furthermore, we have verified that histological and biochemical evidence of postinjury neuropathology is present in a mild injury consistent with established injury severity classification guidelines from the CDC and DoD, despite a lack of acute gross motor or short-term memory deficits. With the recent report of a correlation between low-level blast exposure, serum and CSF biochemical changes, decreased neurocognitive performance, and increased self-reported symptoms in humans[73] as well as other reports that link mBINT to neurodegenerative disease patterns[32,52] and neuropsychiatric sequelae,[9,13,15,70] it is imperative that intensive efforts be made to further explore the relationships among the initial blast injury, secondary biochemical mediators, and long-term changes in brain function in the controlled, reproducible setting of animal models. The data shown here demonstrate anatomical, behavioral, and biochemical metrics used to evaluate the clinical relevance and severity of our injury model, each of which mimics key elements of the human condition. However, our model merits further analysis using a varied number, orientation, and severity of BINT, as well as a more intensive time-course analysis of the observed changes. This model has also provided a framework for evaluating oxidative stress and neuroinflammation-related changes in BINT, particularly those mediated by acrolein, and subsequent work will pursue this for evaluation of diagnostic and therapeutic approaches. Considering the benefit of acrolein scavenging treatment in several other CNS traumas and diseases,[35,42,74,78] it is expected that acrolein may eventually have utility as a theranostic biomarker facilitating more timely medical intervention with novel effective treatment(s) for BINT.

ABBREVIATIONS

3-HPMA	S-(3-hydroxypropyl)mercapturic acid
BBB	blood-brain barrier
BINT	blast-induced neurotrauma
CDC	Centers for Disease Control and Prevention
DiI	di-alkylindocarbocyanine
DoD	Department of Defense
EB	Evans Blue
FO	familiar object
LC-MS/MS	liquid chromatography with tandem mass spectrometry
LOC	loss of consciousness
mBINT	mild BINT
NO	novel object
NOR	novel object recognition
PBS	phosphate-buffered saline
PBST	PBS with Tween 20
PET	polyethylene terephthalate
PTSD	posttraumatic stress disorder

References

1. Abdul-Muneer PM, Schuetz H, Wang F, Skotak M, Jones J, Gorantla S, et al. Induction of oxidative and nitrosative damage leads to cerebrovascular inflammation in an animal model of mild traumatic brain injury induced by primary blast. Free Radic Biol Med. 2013; 60:282–291. [PubMed: 23466554]
2. Agoston DV, Elsayed M. Serum-based protein biomarkers in blast-induced traumatic brain injury spectrum disorder. Front Neurol. 2012; 3:107. [PubMed: 22783223]
3. Agoston DV, Gyorgy A, Eidelman O, Pollard HB. Proteomic biomarkers for blast neurotrauma: targeting cerebral edema, inflammation, and neuronal death cascades. J Neurotrauma. 2009; 26:901–911. [PubMed: 19397421]
4. Andrè E, Campi B, Materazzi S, Trevisani M, Amadesi S, Massi D, et al. Cigarette smoke-induced neurogenic inflammation is mediated by alpha, beta-unsaturated aldehydes and the TRPA1 receptor in rodents. J Clin Invest. 2008; 118:2574–2582. [PubMed: 18568077]
5. Antunes M, Biala G. The novel object recognition memory: neurobiology, test procedure, and its modifications. Cogn Process. 2012; 13:93–110. [PubMed: 22160349]
6. Argaw AT, Gurfein BT, Zhang Y, Zameer A, John GR. VEGF-mediated disruption of endothelial CLN-5 promotes blood-brain barrier breakdown. Proc Natl Acad Sci U S A. 2009; 106:1977–1982. [PubMed: 19174516]

7. Austin MC, Kalivas PW. Enkephalinergic and GABAergic modulation of motor activity in the ventral pallidum. J Pharmacol Exp Ther. 1990; 252:1370–1377. [PubMed: 2319472]
8. Bass CR, Rafaels KA, Salzar RS. Pulmonary injury risk assessment for short-duration blasts. J Trauma. 2008; 65:604–615. [PubMed: 18784574]
9. Belanger HG, Kretzmer T, Yoash-Gantz R, Pickett T, Tupler LA. Cognitive sequelae of blast-related versus other mechanisms of brain trauma. J Int Neuropsychol Soc. 2009; 15:1–8. [PubMed: 19128523]
10. Bevins RA, Besheer J. Object recognition in rats and mice: a one-trial non-matching-to-sample learning task to study 'recognition memory'. Nat Protoc. 2006; 1:1306–1311. [PubMed: 17406415]
11. Bombardier CH, Fann JR, Temkin NR, Esselman PC, Barber J, Dikmen SS. Rates of major depressive disorder and clinical outcomes following traumatic brain injury. JAMA. 2010; 303:1938–1945. [PubMed: 20483970]
12. Borchers MT, Wesselkamper SC, Deshmukh H, Beckman E, Medvedovic M, Sartor M, et al. The role of T cells in the regulation of acrolein-induced pulmonary inflammation and epithelial-cell pathology. Res Rep Health Eff Inst. 2009; 146:5–29.
13. Bryan CJ, Clemans TA, Hernandez AM, Rudd MD. Loss of consciousness, depression, posttraumatic stress disorder, and suicide risk among deployed military personnel with mild traumatic brain injury. J Head Trauma Rehabil. 2013; 28:13–20. [PubMed: 23076097]
14. Calingasan NY, Uchida K, Gibson GE. Protein-bound acrolein: a novel marker of oxidative stress in Alzheimer's disease. J Neurochem. 1999; 72:751–756. [PubMed: 9930749]
15. Carlson KF, Nelson D, Orazem RJ, Nugent S, Cifu DX, Sayer NA. Psychiatric diagnoses among Iraq and Afghanistan war veterans screened for deployment-related traumatic brain injury. J Trauma Stress. 2010; 23:17–24. [PubMed: 20127725]
16. Centers for Disease Control. Bombings: Injury Patterns and Care. ACEP Clinical and Practice Management; Blast injuries: fact sheets for professionals. (http://www.acep.org/blastinjury/) [Accessed June 5, 2015]
17. Cernak I, Merkle AC, Koliatsos VE, Bilik JM, Luong QT, Mahota TM, et al. The pathobiology of blast injuries and blast-induced neurotrauma as identified using a new experimental model of injury in mice. Neurobiol Dis. 2011; 41:538–551. [PubMed: 21074615]
18. Chang JW, Wachtel SR, Young D, Kang UJ. Biochemical and anatomical characterization of forepaw adjusting steps in rat models of Parkinson's disease: studies on medial forebrain bundle and striatal lesions. Neuroscience. 1999; 88:617–628. [PubMed: 10197780]
19. Cho HJ, Sajja VS, Vandevord PJ, Lee YW. Blast induces oxidative stress, inflammation, neuronal loss and subsequent short-term memory impairment in rats. Neuroscience. 2013; 253:9–20. [PubMed: 23999126]
20. Connell, S., Walls, M., Gao, X., Ambaw, A., Chen, L., Chen, J., et al. Modeling traumatic brain injury using a compressed-gas blast chamber. In: Ding, Y.Peng, Y., Shi, R., editors. 2011 4th International Conference on Biomedical Engineering and Informatics. Vol. 2. Piscataway, NJ: IEEE; 2011. p. 969-972.
21. Davalos D, Ryu JK, Merlini M, Baeten KM, Le Moan N, Petersen MA, et al. Fibrinogen-induced perivascular microglial clustering is required for the development of axonal damage in neuroinflammation. Nat Commun. 2012; 3:1227. [PubMed: 23187627]
22. DePalma RG, Burris DG, Champion HR, Hodgson MJ. Blast injuries. N Engl J Med. 2005; 352:1335–1342. [PubMed: 15800229]
23. Desmoulin GT, Dionne JP. Blast-induced neurotrauma: surrogate use, loading mechanisms, and cellular responses. J Trauma. 2009; 67:1113–1122. [PubMed: 19901677]
24. Deumens R, Blokland A, Prickaerts J. Modeling Parkinson's disease in rats: an evaluation of 6-OHDA lesions of the nigrostriatal pathway. Exp Neurol. 2002; 175:303–317. [PubMed: 12061862]
25. Due MR, Park J, Zheng L, Walls M, Allette YM, White FA, et al. Acrolein involvement in sensory and behavioral hypersensitivity following spinal cord injury in the rat. J Neurochem. 2014; 128:776–786. [PubMed: 24147766]

26. Eckert E, Drexler H, Göen T. Determination of six hydroxyalkyl mercapturic acids in human urine using hydrophilic interaction liquid chromatography with tandem mass spectrometry (HILIC-ESI-MS/MS). J Chromatogr B Analyt Technol Biomed Life Sci. 2010; 878:2506–2514.
27. Elder GA, Dorr NP, De Gasperi R, Gama Sosa MA, Shaughness MC, Maudlin-Jeronimo E, et al. Blast exposure induces post-traumatic stress disorder-related traits in a rat model of mild traumatic brain injury. J Neurotrauma. 2012; 29:2564–2575. [PubMed: 22780833]
28. Esterbauer H, Schaur RJ, Zollner H. Chemistry and biochemistry of 4-hydroxynonenal, malonaldehyde and related aldehydes. Free Radic Biol Med. 1991; 11:81–128. [PubMed: 1937131]
29. Everitt BJ, Parkinson JA, Olmstead MC, Arroyo M, Robledo P, Robbins TW. Associative processes in addiction and reward. The role of amygdala-ventral striatal subsystems. Ann N Y Acad Sci. 1999; 877:412–438. [PubMed: 10415662]
30. Facchinetti F, Amadei F, Geppetti P, Tarantini F, Di Serio C, Dragotto A, et al. Alpha, beta-unsaturated aldehydes in cigarette smoke release inflammatory mediators from human macrophages. Am J Respir Cell Mol Biol. 2007; 37:617–623. [PubMed: 17600310]
31. Garman RH, Jenkins LW, Switzer RC III, Bauman RA, Tong LC, Swauger PV, et al. Blast exposure in rats with body shielding is characterized primarily by diffuse axonal injury. J Neurotrauma. 2011; 28:947–959. [PubMed: 21449683]
32. Goldstein LE, Fisher AM, Tagge CA, Zhang XL, Velisek L, Sullivan JA, et al. Chronic traumatic encephalopathy in blast-exposed military veterans and a blast neurotrauma mouse model. Sci Transl Med. 2012; 4:134ra160.
33. Gyorgy A, Ling G, Wingo D, Walker J, Tong L, Parks S, et al. Time-dependent changes in serum biomarker levels after blast traumatic brain injury. J Neurotrauma. 2011; 28:1121–1126. [PubMed: 21428721]
34. Hamann K, Durkes A, Ouyang H, Uchida K, Pond A, Shi R. Critical role of acrolein in secondary injury following ex vivo spinal cord trauma. J Neurochem. 2008; 107:712–721. [PubMed: 18710419]
35. Hamann K, Nehrt G, Ouyang H, Duerstock B, Shi R. Hydralazine inhibits compression and acrolein-mediated injuries in ex vivo spinal cord. J Neurochem. 2008; 104:708–718. [PubMed: 17995940]
36. Hamann K, Shi R. Acrolein scavenging: a potential novel mechanism of attenuating oxidative stress following spinal cord injury. J Neurochem. 2009; 111:1348–1356. [PubMed: 19780896]
37. Hawkins BT, Egleton RD. Fluorescence imaging of blood-brain barrier disruption. J Neurosci Methods. 2006; 151:262–267. [PubMed: 16181683]
38. Ikemoto S. Dopamine reward circuitry: two projection systems from the ventral midbrain to the nucleus accumbensolfactory tubercle complex. Brain Res Brain Res Rev. 2007; 56:27–78.
39. Jang AS, Concel VJ, Bein K, Brant KA, Liu S, Pope-Varsalona H, et al. Endothelial dysfunction and claudin 5 regulation during acrolein-induced lung injury. Am J Respir Cell Mol Biol. 2011; 44:483–490. [PubMed: 20525806]
40. Kirkham PA, Spooner G, Ffoulkes-Jones C, Calvez R. Cigarette smoke triggers macrophage adhesion and activation: role of lipid peroxidation products and scavenger receptor. Free Radic Biol Med. 2003; 35:697–710. [PubMed: 14583334]
41. Koob AO, Cirillo J, Babbs CF. A novel open field activity detector to determine spatial and temporal movement of laboratory animals after injury and disease. J Neurosci Methods. 2006; 157:330–336. [PubMed: 16735064]
42. Leung G, Sun W, Zheng L, Brookes S, Tully M, Shi R. Antiacrolein treatment improves behavioral outcome and alleviates myelin damage in experimental autoimmune encephalomyelitis mouse. Neuroscience. 2011; 173:150–155. [PubMed: 21081153]
43. Li Y, Song Y, Zhao L, Gaidosh G, Laties AM, Wen R. Direct labeling and visualization of blood vessels with lipophilic carbocyanine dye DiI. Nat Protoc. 2008; 3:1703–1708. [PubMed: 18846097]
44. Loane DJ, Byrnes KR. Role of microglia in neurotrauma. Neurotherapeutics. 2010; 7:366–377. [PubMed: 20880501]

45. Lovell MA, Xie C, Markesbery WR. Acrolein is increased in Alzheimer's disease brain and is toxic to primary hippocampal cultures. Neurobiol Aging. 2001; 22:187–194. [PubMed: 11182468]
46. Luethcke CA, Bryan CJ, Morrow CE, Isler WC. Comparison of concussive symptoms, cognitive performance, and psychological symptoms between acute blast-versus nonblast-induced mild traumatic brain injury. J Int Neuropsychol Soc. 2011; 17:36–45. [PubMed: 21083963]
47. Luo J, Robinson JP, Shi R. Acrolein-induced cell death in PC12 cells: role of mitochondria-mediated oxidative stress. Neurochem Int. 2005; 47:449–457. [PubMed: 16140421]
48. Luo J, Shi R. Acrolein induces axolemmal disruption, oxidative stress, and mitochondrial impairment in spinal cord tissue. Neurochem Int. 2004; 44:475–486. [PubMed: 15209416]
49. Luo J, Shi R. Acrolein induces oxidative stress in brain mitochondria. Neurochem Int. 2005; 46:243–252. [PubMed: 15670641]
50. Luo J, Uchida K, Shi R. Accumulation of acrolein-protein adducts after traumatic spinal cord injury. Neurochem Res. 2005; 30:291–295. [PubMed: 16018572]
51. Maguen S, Lau KM, Madden E, Seal K. Relationship of screen-based symptoms for mild traumatic brain injury and mental health problems in Iraq and Afghanistan veterans: Distinct or overlapping symptoms? J Rehabil Res Dev. 2012; 49:1115–1126. [PubMed: 23341283]
52. Miller G. Blast injuries linked to neurodegeneration in veterans. Science. 2012; 336:790–791. [PubMed: 22605724]
53. Moretto N, Facchinetti F, Southworth T, Civelli M, Singh D, Patacchini R. α,β-Unsaturated aldehydes contained in cigarette smoke elicit IL-8 release in pulmonary cells through mitogen-activated protein kinases. Am J Physiol Lung Cell Mol Physiol. 2009; 296:L839–L848. [PubMed: 19286926]
54. Nitta T, Hata M, Gotoh S, Seo Y, Sasaki H, Hashimoto N, et al. Size-selective loosening of the blood-brain barrier in claudin-5-deficient mice. J Cell Biol. 2003; 161:653–660. [PubMed: 12743111]
55. Okie S. Traumatic brain injury in the war zone. N Engl J Med. 2005; 352:2043–2047. [PubMed: 15901856]
56. Ouyang H, Galle B, Li J, Nauman E, Shi R. Biomechanics of spinal cord injury: a multimodal investigation using ex vivo guinea pig spinal cord white matter. J Neurotrauma. 2008; 25:19–29. [PubMed: 18355155]
57. Ouyang H, Sun W, Fu Y, Li J, Cheng JX, Nauman E, et al. Compression induces acute demyelination and potassium channel exposure in spinal cord. J Neurotrauma. 2010; 27:1109–1120. [PubMed: 20373847]
58. Park J, Zheng L, Marquis A, Walls M, Duerstock B, Pond A, et al. Neuroprotective role of hydralazine in rat spinal cord injury-attenuation of acrolein-mediated damage. J Neurochem. 2014; 129:339–349. [PubMed: 24286176]
59. Park YS, Taniguchi N. Acrolein induces inflammatory response underlying endothelial dysfunction: a risk factor for atherosclerosis. Ann N Y Acad Sci. 2008; 1126:185–189. [PubMed: 18448814]
60. Pocernich CB, Cardin AL, Racine CL, Lauderback CM, Butterfield DA. Glutathione elevation and its protective role in acrolein-induced protein damage in synaptosomal membranes: relevance to brain lipid peroxidation in neurodegenerative disease. Neurochem Int. 2001; 39:141–149. [PubMed: 11408093]
61. Ravikumar M, Sunil S, Black J, Barkauskas DS, Haung AY, Miller RH, et al. The roles of blood-derived macrophages and resident microglia in the neuroinflammatory response to implanted intracortical microelectrodes. Biomaterials. 2014; 35:8049–8064. [PubMed: 24973296]
62. Rosenfeld JV, McFarlane AC, Bragge P, Armonda RA, Grimes JB, Ling GS. Blast-related traumatic brain injury. Lancet Neurol. 2013; 12:882–893. [PubMed: 23884075]
63. Sasaki Y, Ohsawa K, Kanazawa H, Kohsaka S, Imai Y. Iba1 is an actin-cross-linking protein in macrophages/microglia. Biochem Biophys Res Commun. 2001; 286:292–297. [PubMed: 11500035]
64. Sayer NA, Chiros CE, Sigford B, Scott S, Clothier B, Pickett T, et al. Characteristics and rehabilitation outcomes among patients with blast and other injuries sustained during the Global War on Terror. Arch Phys Med Rehabil. 2008; 89:163–170. [PubMed: 18164349]

65. Shi R, Luo J, Peasley M. Acrolein inflicts axonal membrane disruption and conduction loss in isolated guinea-pig spinal cord. Neuroscience. 2002; 115:337–340. [PubMed: 12421600]
66. Shi R, Luo J. The role of acrolein in spinal cord injury. Appl Neurol. 2006; 2:22–27.
67. Shi R, Rickett T, Sun W. Acrolein-mediated injury in nervous system trauma and diseases. Mol Nutr Food Res. 2011; 55:1320–1331. [PubMed: 21823221]
68. Skotak M, Wang F, Alai A, Holmberg A, Harris S, Switzer RC, et al. Rat injury model under controlled field-relevant primary blast conditions: acute response to a wide range of peak overpressures. J Neurotrauma. 2013; 30:1147–1160. [PubMed: 23362798]
69. Smith KS, Tindell AJ, Aldridge JW, Berridge KC. Ventral pallidum roles in reward and motivation. Behav Brain Res. 2009; 196:155–167. [PubMed: 18955088]
70. Spikman JM, Timmerman ME, Milders MV, Veenstra WS, van der Naalt J. Social cognition impairments in relation to general cognitive deficits, injury severity, and prefrontal lesions in traumatic brain injury patients. J Neurotrauma. 2012; 29:101–111. [PubMed: 21933011]
71. Stein L, Wise CD. Release of norepinephrine from hypothalamus and amygdala by rewarding medial forebrain bundle stimulation and amphetamine. J Comp Physiol Psychol. 1969; 67:189–198. [PubMed: 4306672]
72. Svetlov SI, Larner SF, Kirk DR, Atkinson J, Hayes RL, Wang KK. Biomarkers of blast-induced neurotrauma: profiling molecular and cellular mechanisms of blast brain injury. J Neurotrauma. 2009; 26:913–921. [PubMed: 19422293]
73. Tate CM, Wang KK, Eonta S, Zhang Y, Carr W, Tortella FC, et al. Serum brain biomarker level, neurocognitive performance, and self-reported symptom changes in soldiers repeatedly exposed to low-level blast: a breacher pilot study. J Neurotrauma. 2013; 30:1620–1630. [PubMed: 23687938]
74. Tully M, Shi R. New insights in the pathogenesis of multiple sclerosis—role of acrolein in neuronal and myelin damage. Int J Mol Sci. 2013; 14:20037–20047. [PubMed: 24113583]
75. VandeVord, PJ. Measuring Intracranial Pressure and Correlation with Severity of Blast Traumatic Brain Injury. Fort Detrick, MD: US Army Medical Research and Materiel Command; 2013.
76. VandeVord PJ, Bolander R, Sajja VS, Hay K, Bir CA. Mild neurotrauma indicates a range-specific pressure response to low level shock wave exposure. Ann Biomed Eng. 2012; 40:227–236. [PubMed: 21994066]
77. Vilhardt F. Microglia: phagocyte and glia cell. Int J Biochem Cell Biol. 2005; 37:17–21. [PubMed: 15381143]
78. Wood PL, Khan MA, Moskal JR, Todd KG, Tanay VA, Baker G. Aldehyde load in ischemia-reperfusion brain injury: neuroprotection by neutralization of reactive aldehydes with phenelzine. Brain Res. 2006; 1122:184–190. [PubMed: 17026969]
79. Yeoh S, Bell ED, Monson KL. Distribution of blood-brain barrier disruption in primary blast injury. Ann Biomed Eng. 2013; 41:2206–2214. [PubMed: 23568152]
80. Zheng L, Park J, Walls M, Tully M, Jannasch A, Cooper B, et al. Determination of urine 3-HPMA, a stable acrolein metabolite in a rat model of spinal cord injury. J Neurotrauma. 2013; 30:1334–1341. [PubMed: 23697633]

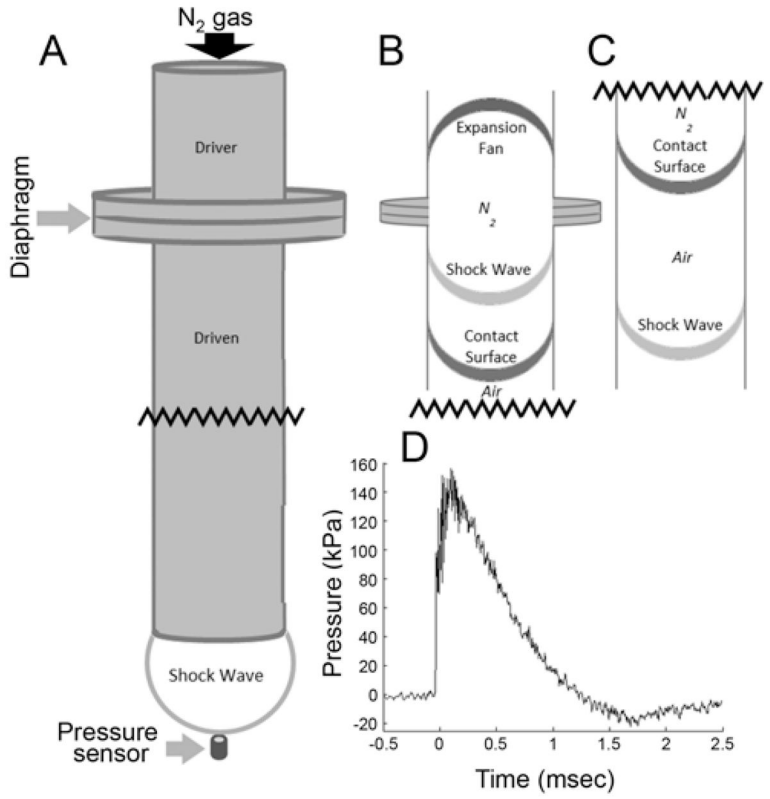

FIG. 1.

Shock wave delivery apparatus. **A:** The shock tube is composed of a driver section (behind the diaphragm where gas is compressed) and a driven section (in front of the diaphragm at atmospheric pressure). For characterization purposes, pressure sensors were positioned within (not depicted) and outside the tube. **B:** After the diaphragm ruptures, the contact surface is initially ahead of the shock wave. **C:** After traveling a significant distance down the length of the tube, the shock wave outpaces the contact surface and is eventually emitted from the open end of the shock tube, where it strikes the head of the rat positioned a distance equivalent to the shock tube inner diameter for optimal blast conditions (same location as the depicted pressure sensor). **D:** Representative shock wave recording exhibiting characteristics of an idealized Fried-lander waveform with a rise time of 0.15 msec, maximum overpressure of 150 kPa, overpressure duration of 1.25 msec, maximum underpressure of 20 kPa, and an underpressure duration of 1.25 msec. Waveform properties are tunable by adjusting thickness of the diaphragm and sensor/subject distance from the open end of the shock tube.

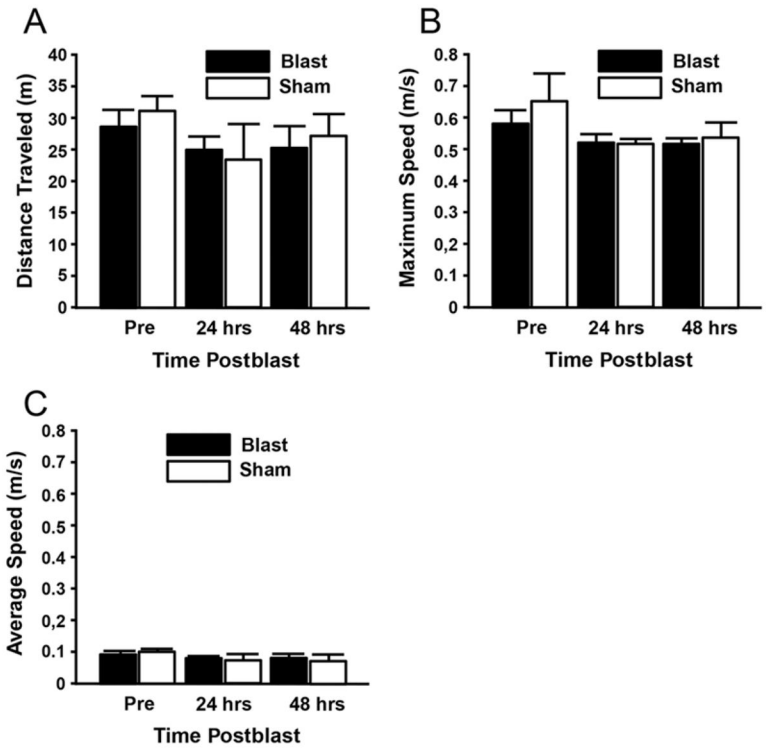

FIG. 2.

Behavioral analysis of motor function in an open-field activity box indicated no significant effects of injury group or day on gross motor activity at 24 or 48 hours postblast. Analyses included distance traveled **(A)**, maximum speed **(B),** and average speed **(C)** ($p > 0.05$, Tukey-Kramer test; n = 4/group). Pre = preblast.

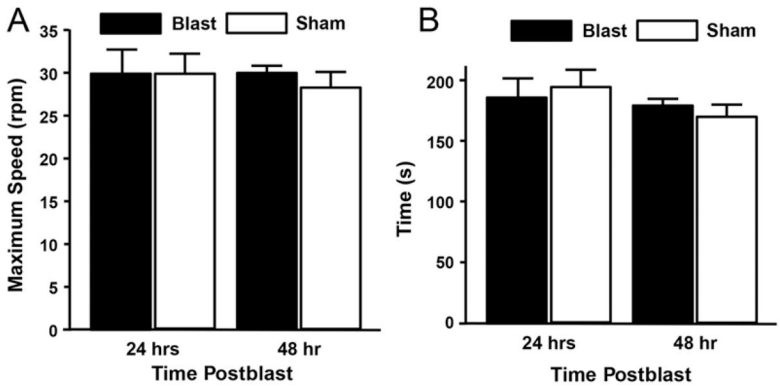

FIG. 3.

Behavioral analysis of motor function in rotarod testing indicated no significant effects of injury group or day at 24 or 48 hours postblast. Criteria were maximum speed **(A)** and total run time **(B)** ($p > 0.05$, Tukey-Kramer test; n = 4/group).

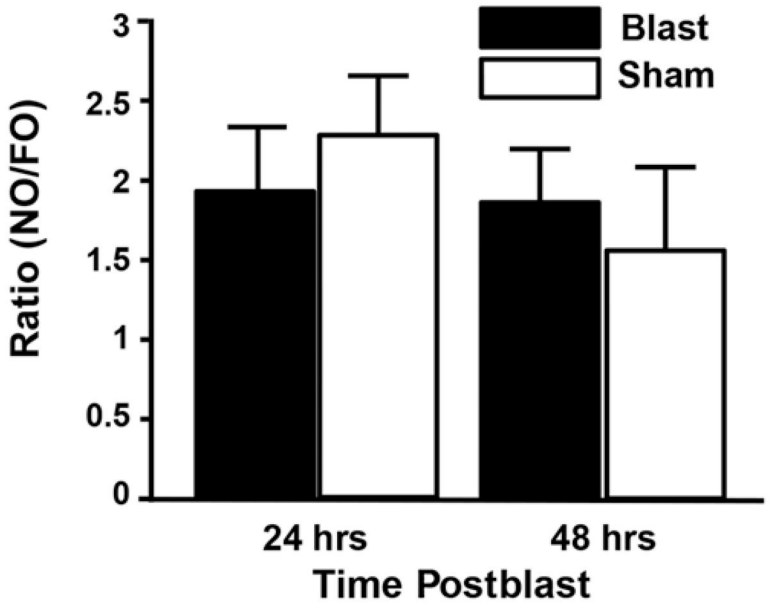

FIG. 4.

Behavioral analysis of NOR indicated no significant effects of injury group or day on short-term memory function at 24 or 48 hours postblast. Both blast-exposed and sham-injured rats showed intact NOR with the ability to consistently distinguish NO from FO with an NO/FO ratio of approximately 2:1 ($p > 0.05$, Tukey-Kramer test; $n = 4$/group).

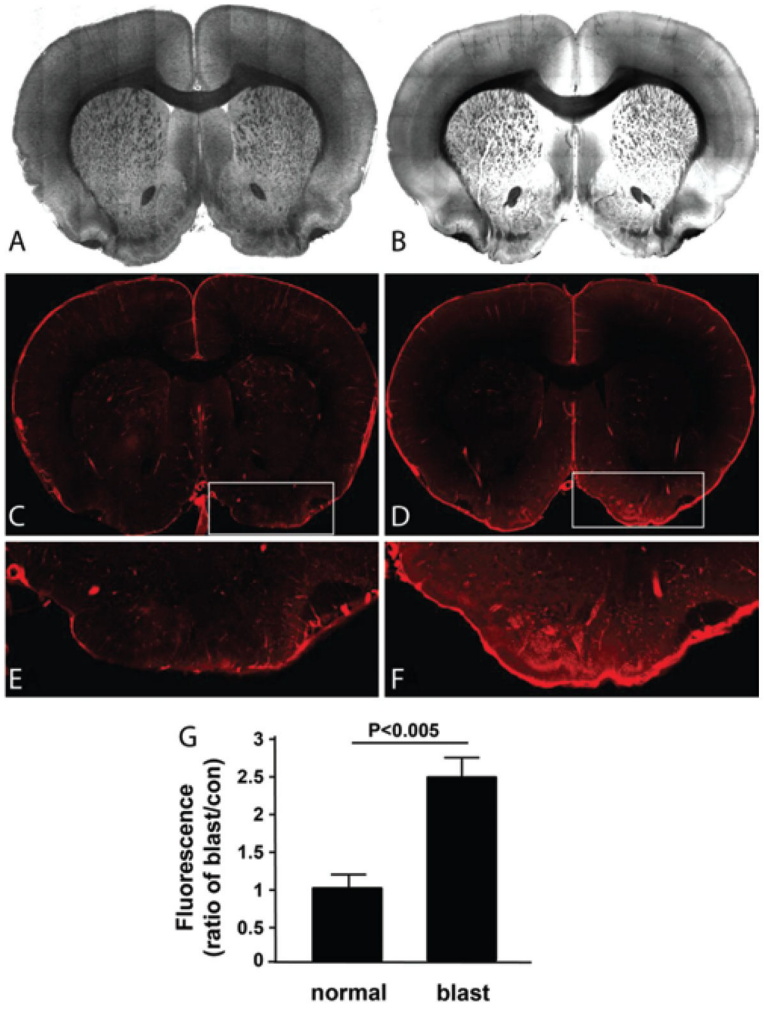

FIG. 5.

Extravasation of serum albumin analysis by EB fluorescence imaging indicated damage to the BBB. Control sections, that is, no blast exposure **(A, C, and E)**. Blast-exposed tissue sections **(B, D, and F)**. The blast-injured tissue shows elevated fluorescence that is most pronounced in the ventral aspects of the section. This fluorescence indicates the presence of extravascular serum albumin bound to EB that escaped vessels as a result of the blast-damaged microvasculature. Quantification **(G)** of the average fluorescence in control and blast-exposed tissues in the ventral region of interest (E and F, enlarged insets in panels C and D, respectively). The fluorescence intensity in blast-exposed rats is significantly higher than that in sham-injured rats ($p < 0.005$, Student t-test; $n = 4$/group). Figure is available in color online only.

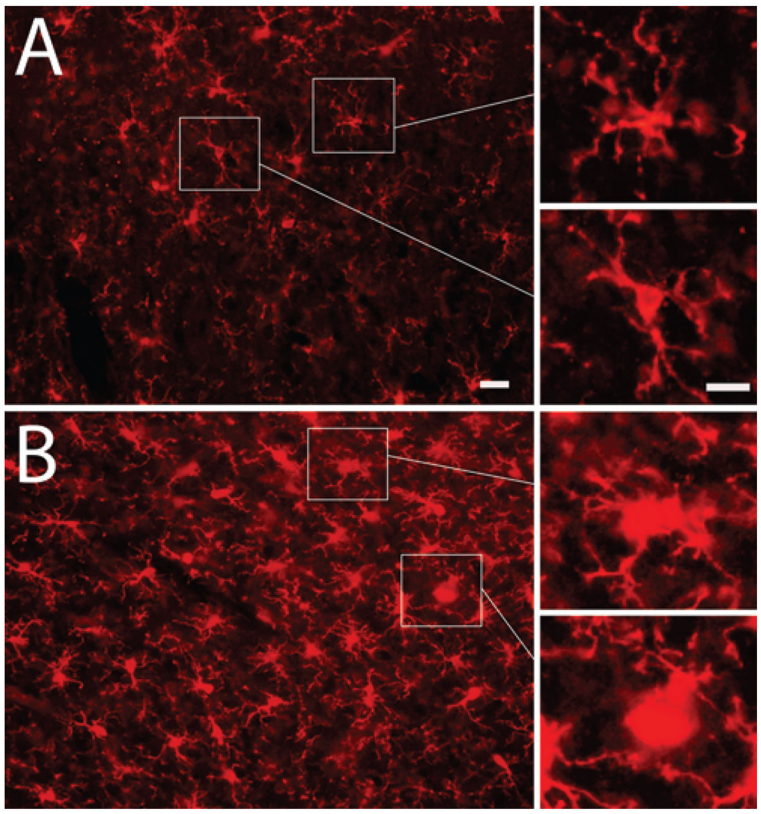

FIG. 6.

Immunohistochemical assessment of microglial/macrophage activation. Representative image of 25-μm-thick coronal sections of sham-injured and blast-injured rat brains after immunofluorescence staining for the microglial/macrophage marker Iba1 *(red)* indicating glial activation or macrophage infiltration. Sham-injured sections **(A)**. Blast-injured tissue sections **(B)**. All images correspond to ventral areas of interest from Fig. 5E and F. Digitally zoomed insets (right) highlight the characteristic amoeboid, “activated” morphology of Iba-1+ cells after mBINT (B) as compared with the stellate, “resting state” morphology of Iba-1+ cells in sham-injured animals (A). Bar = 10 μm (A and B) and 5 μm (insets). Figure is available in color online only.

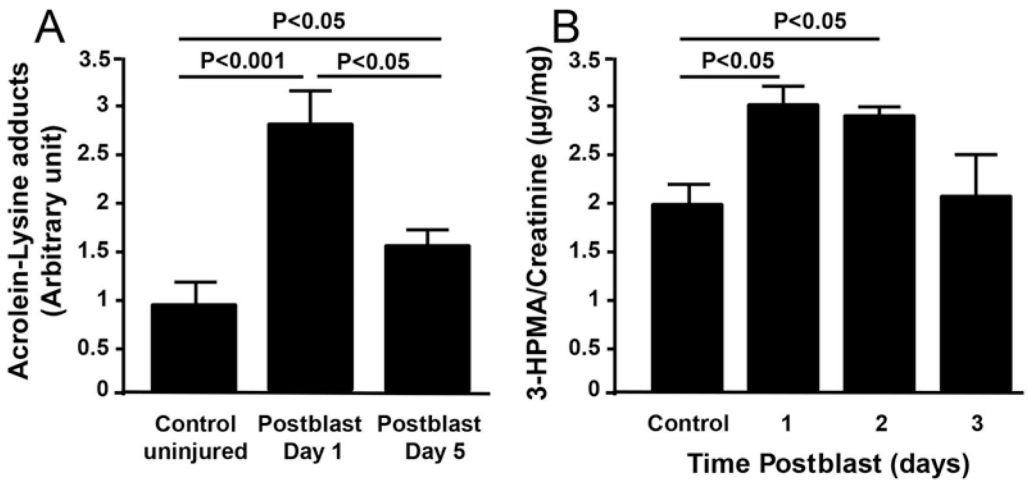

FIG. 7.

Biochemical markers for tissue and cellular stress. **A:** Acrolein-lysine adducts in the brain tissue at 1 (Day 1) and 5 (Day 5) days postblast were detected via dot blot analysis. The acrolein-lysine level of both Day 1 and Day 5 are significantly elevated when compared with levels in preblast controls ($p < 0.001$ and $p < 0.05$, respectively, Tukey-Kramer test; $n = 5$ rats/group). In addition, the acrolein-lysine level of Day 1 is significantly higher than that of Day 5 ($p < 0.05$, Tukey-Kramer test; $n = 5$ rats/group). **B:** Urine 3-HPMA detected by LC-MS/MS relative to urine creatinine content. Urine was collected for 3 days postblast, indicating significant elevation of 3-HPMA in the first 2 days following exposure as compared with preexposure levels ($p < 0.05$, Tukey-Kramer test; $n = 5$ rats).